Pixel-wise Ground Truth Annotation in Videos
An Semi-automatic Approach for Pixel-wise and Semantic Object Annotation

Julius Schöning, Patrick Faion and Gunther Heidemann
Institute of Cognitive Science, University of Osnabrück, Osnabrück, Germany

Keywords: Semantic Ground Truth Annotation, Video Annotation, Polygon Shaped, Semi-automatic.

Abstract: In the last decades, a large diversity of automatic, semi-automatic and manual approaches for video segmentation and knowledge extraction from video-data has been proposed. Due to the high complexity in both the spatial and temporal domain, it continues to be a challenging research area. In order to develop, train, and evaluate new algorithms, ground truth of video-data is crucial. Pixel-wise annotation of ground truth is usually time-consuming, does not contain semantic relations between objects and uses only simple geometric primitives. We provide a brief review of related tools for video annotation, and introduce our novel interactive and semi-automatic segmentation tool *iSeg*. Extending an earlier implementation, we improved *iSeg* with a semantic time line, multithreading and the use of ORB features. A performance evaluation of *iSeg* on four data sets is presented. Finally, we discuss possible opportunities and applications of semantic polygon-shaped video annotation, such as 3D reconstruction and video inpainting.

1 INTRODUCTION

If YouTube would be watching and annotating all uploaded videos manually and in real time, 18,000 operators would be necessary. This number is based on the official press statistics of YouTube (2015), where YouTube stated that 300 hours of video are uploaded every minute just to their platform. Thus, knowledge extraction, knowledge acquisition, and semantic scene understanding from video-data is important. Detection of concepts such as "person", "building" or "car" is possible by current automatic content analysis in many cases, provided there is no occulsion (Dasiopoulou et al., 2011; Höferlin et al., 2015; Tanisaro et al., 2015). So manually created annotations become ever more important because they are necessary as ground truth for the development of algorithms—both for training and evaluation.

In the architecture of video visual analytics (VVA) by Tanisaro et al. (2015) the computer assists the user on the two lowest levels of the reasoning process: the *extraction of meaningful artifacts* and the *assessment of situations*. All annotation methods for video and image data, mentioned by Dasiopoulou et al. (2011), do no use such interactive techniques. Following the VVA architecture of combining the computational power of a computer with the high level abilities of the human user, we (Schöning et al., 2015) designed *iSeg*. Through *iSeg*'s semi-automatic design the quality of the results increases significantly with a slight improvement in the annotation speed.

While current freely available video annotation tools (Doermann and Mihalcik, 2000; Wu et al., 2014; Yao et al., 2012) usually provide only simple geometric primitives like rectangles and ellipses, *iSeg* provides polygon-shaped areas—a significant improvement in video annotation. Another problem of current tools is that they provide no or little support for an easy concurrent annotation of several frames. Further, they do not provide means to enter semantic inter-object knowledge, like "the blue car is in front of the yellow house".

To overcome these drawbacks, we propose an interactive, semi-automatic process based on polygons. Arbitrary polygonal shapes can be annotated, and the user is actively asked for interaction if the result of the automatic annotation process seems to be incorrect. Compared to a previous version of *iSeg*, we accomplished a major improvement of the user interface (UI): The semantic time line provides intuitive and easy to use interaction metaphors for authoring semantic knowledge. Another improvement has been made in the user experience, where efficient multithreading implementations minimize the system's response time and allow the user to interact with the system, while time-consuming tasks run on a differ-

Schöning, J., Faion, P. and Heidemann, G.
Pixel-wise Ground Truth Annotation in Videos - An Semi-automatic Approach for Pixel-wise and Semantic Object Annotation.
DOI: 10.5220/0005823306900697
In *Proceedings of the 5th International Conference on Pattern Recognition Applications and Methods (ICPRAM 2016)*, pages 690-697
ISBN: 978-989-758-173-1

ent process. Finally, we were able to reduce the processing time needed for automatic contour tracking by using ORB features instead of SIFT features.

2 STATE OF THE ART

Using criteria like in- and output formats, metadata types, as well as granularity, localization, and expressivity of the annotations, Dasiopoulou et al. (2011) reviewed and compared several image and video annotation tools. According to their review, four of seven image annotation tools provide polygon-shaped annotations, but in contrast only one of seven video annotation tools provides polygon-shaped annotations, the Video and Image Annotation tool (*VIA*) (Multimedia Knowledge and Social Media Analytics Laboratory, 2015). But during testing the latest version *VIA* (Version 1.0s), we were able to annotate frames by rectangular areas only. Unfortunately, we were unable to annotate polygon-shaped areas, because we did not find any other non-rectangular annotation marker in the user interface. We also noticed that *VIA* only displays a clipped region of a FullHD video.

In 2000, Doermann and Mihalcik (2000) developed the Video Performance Evaluation Resource (*ViPER*). An automatic 2D propagation of the annotated object can be used to speed up the annotation process. This tool is still quite popular, due to its properly defined and specified *XML* output format. The specified *XSD* schema of the *XML* output is still a basic of a straightforward usage of *ViPER*'s annotations for other applications.

Wu et al. (2014) designed the Semi-Automatic Ground Truth Annotation tool (*SAGTA*) for the rectangular annotation of pedestrians in scenes. Its semi-automatic process relies on the assumption of 3D linear motion supported by ORB feature matching. It reduces the number of manually annotated frames. Because of the 3D linear motion assumption, the input video for *SAGTA* must be taken by fixed cameras, e.g., surveillance cameras.

Using the crowd for performing annotations in real-time, the Vannotea System (Schroeter et al., 2003) pool the resources of several users. This still exotic approach enables multiple users to index, browse, annotate and discuss the same video sequences at the same time.

3 iSeg

Based on the architecture of VVA, *iSeg* focused on a semi-automatic process that puts the user into the loop. As shown in Figure 1, *iSeg* consists of eight main process blocks. Two blocks of these eight are obligatory and must be processed in a specific order—in Figure 1 marked with a white headline—but the remaining process blocks—in Figure 1 marked with a gray headline—can be executed by the user in any sequence. These blocks can also be repeated as often as necessary until the intended annotation is achieved.[1]

The first obligatory process block is the selection of the video or the image sequence by the user. The second obligatory process block is marking one or more areas of interest (AOI) in at least two frames by the user, e.g., in the first frame the AOI appears and in the last frame the AOI disappears. In addition, the user can optionally identify the AOI in every frame between these two frames. The following process steps from the *automatic morphing process of the polygon geometry* via the *interactive semi-automatic AOI fitting* to the *export of the resulting annotations* are now described in detail.

3.1 Polygon Morphing

Since the user is identifying the AOI only on a few frames, the algorithm has to estimate the positions and the contours of the AOI on the intermediate frames. For convenience, the user can use polygons with varying numbers of vertices on different frames. Contours of common AOI can be both convex or concave, are intersection free, and, for simplicity, holes in the AOI are omitted. Thus the task is to morph two *simple polygons*, i.e., non self-intersecting ones with different numbers of vertices. Additionally, it is important that all intermediate polygons are also *simple polygons*, since they resemble the contours as well.

There are several existing algorithms in the literature concerning polygon interpolation. One of the first is the Cobos and Peetre (1991) polygon interpolation, unfortunately, it works only with convex polygons. Alt and Guibas (1996) gave a short overview of other approaches but already stated that morphing simple polygons is rather complex when all intermediate polygons need to be simple as well. Most approaches, especially those matching polygonal chains, will usually result in self-intersecting intermediate polygons. There is also a promising method by Gotsman and Surazhsky (2001) on morphing even polygons with holes, but it requires the polygons to have the same number of vertices. So, given our constraints, the problem is non-trivial. In addition, we found that approaches with a direct vertex-to-vertex mapping will often result in artificial rotation

[1]Demonstration video of the annotation process *iSeg* https://ikw.uos.de/∼cv/publications/icpram15

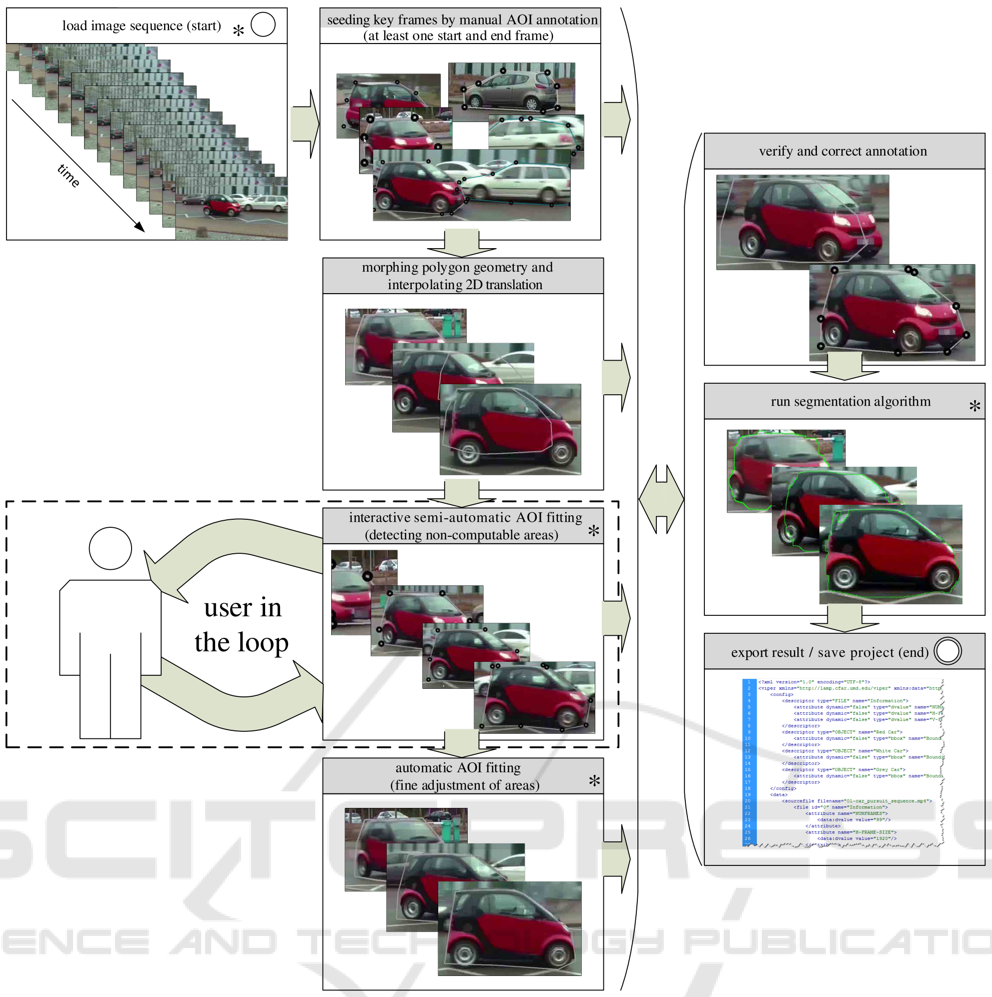
load image sequence (start)
time
seeding key frames by manual AOI annotation (at least one start and end frame)
morphing polygon geometry and interpolating 2D translation
interactive semi-automatic AOI fitting (detecting non-computable areas)
user in the loop
automatic AOI fitting (fine adjustment of areas)
verify and correct annotation
run segmentation algorithm
export result / save project (end)

```
<?xml version="1.0" encoding="UTF-8"?>
<viper xmlns="http://lamp.cfar.umd.edu/viper" xmlns:data="http
    <config>
        <descriptor type="FILE" name="Information">
            <attribute dynamic="false" type="dvalue" name="NUM
            <attribute dynamic="false" type="dvalue" name="H-F
            <attribute dynamic="false" type="dvalue" name="V-F
        </descriptor>
        <descriptor type="OBJECT" name="Red Car">
            <attribute dynamic="false" type="bbox" name="Bound
        </descriptor>
        <descriptor type="OBJECT" name="White Car">
            <attribute dynamic="false" type="bbox" name="Boundi
        </descriptor>
        <descriptor type="OBJECT" name="Grey Car">
            <attribute dynamic="false" type="bbox" name="Bound
        </descriptor>
    </config>
    <data>
        <sourcefile filename="01-car_pursuit_sequence.mp4">
            <file id="0" name="Information">
                <attribute name="NUMFRAMES">
                    <data:dvalue value="99"/>
                </attribute>
                <attribute name="H-FRAME-SIZE">
                    <data:dvalue value="1920"/>
```

Figure 1: Process overview of *iSeg*'s interactive semi-automatic annotation and segmentation process. Process blocks with white headlines are obligatory to run *iSeg*. Blocks with gray headlines are optional and can be used in any order at any time. The process block *interactive SIFT key point fitting* actively asks for user interaction in case the automatically generated annotations appear to be incorrect. Thus, the computer remains the "work horse" of the process, while the close cooperation with the user allows *iSeg* to achieve sophisticated results. The system response time in blocks marked with "*" is minimized using multithreading.

of the contour. However, computer vision can detect the relative rotation of an object between frames, e.g., using the rotation information in the scale-invariant feature transform (SIFT) (Lowe, 2004). Therefore, the rotational component could be separated and vertex morphing should be approximately radial. Since none of the existing methods seemed to fit our needs, we implemented a new, very basic form of polygon matching to test whether the semi-automatic approach with the aid of computer vision is viable.

Given two polygons $\mathcal{A} = \{a_1, a_2, ..., a_n\}$ and $\mathcal{B} = \{b_1, b_2, ..., b_m\}$ we first separate out the translation component by centering the polygons on their center of gravity. In the future, we would also like to extract a rotation component beforehand by means of computer vision. To cope with the problem of different vertex numbers, we introduce additional points in the polygons. For every point in $\mathcal{A}$ there will be an additional point on the contour of $\mathcal{B}$ and vice versa, so all intermediate polygons will have $n+m$ points. For every point $a_i \in \mathcal{A}$ the position of the matching additional point on the contour of $\mathcal{B}$ is the point on the contour with the smallest distance to $\mathcal{A}$: $match(a_i) = \arg\min_{c_i \in \pi(a_i)}(||a_i - c_i||)$ where $\pi(a_i)$ is the set of closest points to a_i on every line segment in $\mathcal{B}$. The points a_i and $match(b_j)$ (as well as b_j and $match(a_i)$) will then be collected into two new polygons according to their positions in $\mathcal{A}$ and $\mathcal{B}$. As a result, there are $n+m$ points on the contour of $\mathcal{A}$ and $n+m$ points on the contour of $\mathcal{B}$, where each point from the contour of $\mathcal{A}$ matches to a corresponding point on the contour of $\mathcal{B}$ and vice versa.

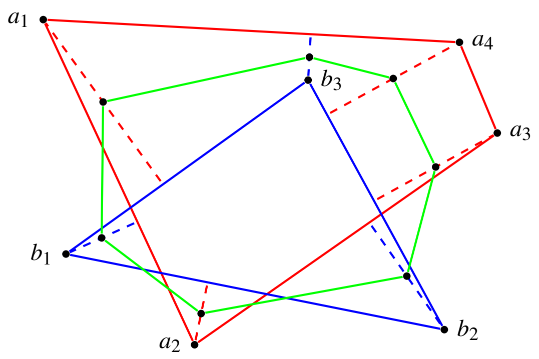

Figure 2: Visualization of polygon morphing between polygon $\mathcal{A}$ (red) and polygon $\mathcal{B}$ (blue). Dashed lines indicate the matching between each polygon point and the closest corresponding point on the other polygon. The green polygon is an intermediate interpolation at $t = 0.5$.

Unfortunately, there can be cases where predecessor-successor relations are violated. Checking the order of vertices in $\mathcal{A}$ and $\mathcal{B}$ and exchanging conflicting vertices can correct some of these violations. Finally we interpolate linearly between matched points as well as along the translation vector. A visualization of the pure shape morphing can be seen in Figure 2.

The algorithm is very simple and straightforward. It already works in many cases, especially when the two polygons are not completely different in their shape, which will be the common case in this context. Still, it is only a "heuristic" approach and there are problems with some polygons where the point matching is not possible such that predecessor-successor relations are preserved. In these cases, there can be self-intersecting polygons on intermediate frames. Nevertheless, this first approach can deal with polygons with different numbers of vertices and in principle also with concave polygons—although they are more likely to cause errors. In addition, the matching of points straight onto the closest corresponding point does not introduce unjustified rotations. With time complexity $O(nm)$, the algorithm is rather fast. We are aware that our approach is still at an early stage and might not be adjustable to work without errors in all situations. But due to the lack of existing methods suiting our requirements, it is a first step into a field with further research potential.

3.2 Interactive Semi-automatic AOI Fitting

Within this process block the linearly interpolated intermediary polygons of the AOI will be adjusted to fit the real object on each frame. This is necessary, since the 2D-projection of the real movement of the AOI will most likely be non-linear in reality. Therefore, the *oriented FAST and rotated BRIEF* (ORB) algorithm by Rublee et al. (2011) is applied to the AOI to extract z key points $\mathcal{F} = \{f_1, f_2, ..., f_z\}$ of each $AOI_1, AOI_2, ..., AOI_y$. Note, to minimize the computational cost of the ORB algorithm, only the inner areas of the AOI are processed—the processing on the whole image increases the computational cost significantly. The ORB algorithm performs as well as SIFT (Lowe, 2004), but with less computational time (Rublee et al., 2011). Thus the system response time, aka the "waiting time" for the user, is minimized.

All key points $\mathcal{F}$ are calculated for the AOI on the current frame $\mathcal{F}_g$ and for the corresponding AOI on the next frame $\mathcal{F}_{(g+1)}$, highlighted with white circles in Figure 4. Under the assumption that rotation and scaling of the object in the AOI are negligible, the key points from the current frame $\mathcal{F}_g$ are matched with the next frame $\mathcal{F}_{(g+1)}$ using FLANN (Muja and Lowe, 2009). Based on the approximate nearest neighbors matching result $\mathcal{M}_{g-(g+1)} = \{m_1, m_2, ..., m_n\}$, key points $f \in \mathcal{F}_g \wedge f \in \mathcal{F}_{(g+1)}$ with distances $\mathcal{M}_{g-(g+1)}$ bigger than 100 are eliminated. In case more than 10 key points of $\mathcal{F}_g$ and $\mathcal{F}_{(g+1)}$ are left after the key point elimination, the centers of gravity of the remaining i key points $C_{\mathcal{F}} = \sum_{c=1}^{i} f_c$ for $\mathcal{F}_g$ and $\mathcal{F}_{(g+1)}$ are calculated, shown as blue points in Figure 4(a). Furthermore, the center of gravity $C_{AOI} = \sum_{c=1}^{n} a_c$ of the AOI polygon in the current and next frame are computed, in Figure 4(a) marked with a gray point. Next the vector $\vec{v} = (C_{\mathcal{F}} - C_{AOI})$ between the center of gravity of the key points and the center of gravity of the AOI is determined. If rotation and scaling are negligible, the vector $\vec{v}$ on the current and on the next frame are approximately the same. Under the assumption that the center of gravity of the key points $C_{\mathcal{F}}$ is congruent to the non-linear movement of the object, a vector can be used to adjust the position of the AOI. Therefore, the new center of gravity of the AOI C'_{AOI} in the next frame is calculated concerning to vector $\vec{v}$ of the current frame. The new center C'_{AOI} is marked as a red point in Figure 4(a). With the difference $\Delta = C_{AOI} - C'_{AOI}$ an affine transformation of the AOI using homogeneous coordinates is performed. As a consequence, the AOI is transformed and the non-linear motion of the AOI is taken into account.

As shown as in Figure 4(b), if less than 10 key points as element of $\mathcal{F}_g$ and $\mathcal{F}_{(g+1)}$ are left after the elimination, the algorithm actively asks the user for interaction. The user can now adjust the polygon AOI with three intuitive metaphors described in Section 3.4 and continue the interactive semi-automatic AOI fitting process. The main reasons for less than

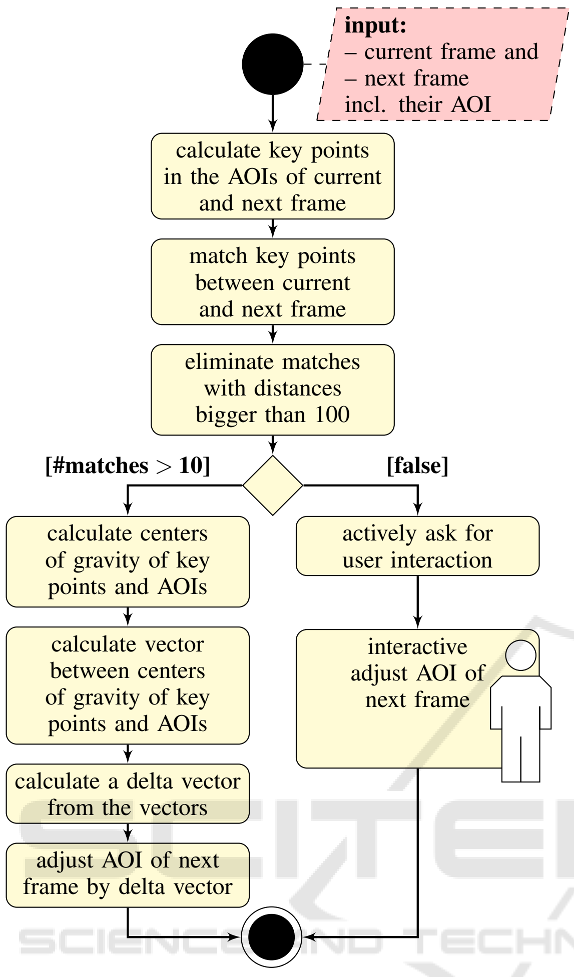
input:
– current frame and
– next frame
incl. their AOI
calculate key points in the AOIs of current and next frame
match key points between current and next frame
eliminate matches with distances bigger than 100
[#matches > 10]
[false]
calculate centers of gravity of key points and AOIs
calculate vector between centers of gravity of key points and AOIs
calculate a delta vector from the vectors
adjust AOI of next frame by delta vector
actively ask for user interaction
interactive adjust AOI of next frame

Figure 3: Activity diagram of the interactive semi-automatic AOI fitting. It has to be repeated until all AOI are adjusted.

10 key points remaining are that the size of the AOI is too small, the AOI is occluded, the AOI mainly contains textureless areas, or the object in the AOI has changed between two frames.

This process of close cooperation between computer and user is continued until all AOI are detected that cannot be computed automatically.

3.3 Automatic AOI Fitting

The automatic AOI runs the same algorithm as the semi-automatic AOI, see Figure 3, but with a slight difference. In case less than 10 key points are left after the elimination, the next frame remains unchanged and the process will be continued. The main idea of this process block is that it is performed after the *interactive semi-automatic AOI fitting* is performed once and has detected all non-automatically computable AOI. On that condition, the automatic AOI fitting increases the accuracy of the result iteration by iteration, because all difficult cases are solved in cooperation with the user.

3.4 AOI Verification and Correction

To verify and correct the result in every stage of the process, the *frame view* provides three intuitive metaphors: i) the relocation of the whole AOI by clicking inside the AOI and dragging the AOI to the designated area, ii) the adjustment of vertices (single click, then drag) and adding vertices (double click between to existing vertices), and iii) the re-creation of the AOI by deleting the vertices and creating new vertices by double-clicking.

3.5 Tailoring of AOI

In computer vision numerous automatic and semi-automatic segmentation algorithms are available (Boykov et al., 2001; Rother et al., 2004; Caselles et al., 1997). Since AOI are marked by a polygon boundary, the semi-automatic *GrabCut* algorithm (Rother et al., 2004) is implemented to tailor the AOI to the real boundaries of the objects. The *GrabCut* algorithm requires a high computational effort, so the response time for the user is much too high to perform it in an interactive dialog as proposed by Rother et al. (2004) for single images. Under the assumption that the available AOI are a good fit to the object boundaries, the *GrabCut* algorithm is initialized with the following information: As possible foreground of the object a rectangular bounding box 1.1 the size of the AOI is used, as explicit foreground of the object a polygon of 0.9% the size of the AOI is set and the remaining area of the image is explicitly set as background. In the current implementation of *iSeg*, the results of *GrabCut* are closely fitting the AOI to the objects, but unfortunately in many cases still the result is not better than the original AOI.

3.6 Save Project and Data Export

At any time the user can save the project. This allows the user to reload the project for later modification of AOI, adding new AOI, or changing semantic information. Beyond saving the project in the *iSeg* data format, the user can export the annotated AOI as *XML* valid to the *XSD* schema of *ViPER* (Doermann and Mihalcik, 2000).

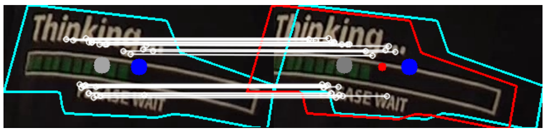

(a) $\geq$ 10 key points – automatic adjustment of the AOI

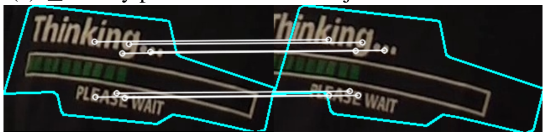

(b) $<$ 10 key points – actively request for interaction

Figure 4: Example of used ORB key points for the AOI fitting. On the left: AOI of current frame; On the right: AOI of next frame; White circles: ORB key points $f_1, f_2, ..., f_z$; White lines: FLANN matches of key points; Blue points: Center of gravity of key points $C_{\mathcal{F}}$; Gray points: Center of gravity of the AOI C_{AOI}; Red point: New center of gravity of the AOI C'_{AOI}.

3.7 User Interface

The UI of *iSeg* consists of four main areas: ⓐ *main context menu*, ⓑ *tool bar*, ⓒ *frame view* and *navigation area*, and ⓓ *semantic time line* as seen in Figure 5. The main context menu includes, as usually, all options which are provided by *iSeg*, including information about the current version. Frequently used tools and functions like *open project*, *semi-automatic AOI fitting*, and *tailor AOI* are also available in the *tool bar*. The manual AOI annotation as well as the interactive AOI adjustment is done within the *frame view* and *navigation area*. For adding semantic information to the annotation, the *semantic time line* provides a bundle of features. To start with the obvious all AOI are listed and color coded in the *semantic time line*. Next to the AOI names different types of lines describe the state of the AOI at this time. Possible states are: i) the AOI is on the current frame and visible – bold line, ii) the AOI is on the current frame and occluded or partially occluded – broken line, iii) the AOI is not on the current frame – light line. In addition, the lines also represent the stack order of the AOI aka z-order. Is an AOI in front of an other AOI, the corresponding line is above the other line. In addition, dots on the lines visualize if an AOI annotation is created manually – big dot, or created automatically – small dot.

3.8 Multithreading

Putting the user in the loop is the central component of *iSeg*. As mentioned by Shneiderman (1984), the response time is a significant value in human-machine interaction, also, the repose time should be minimized. To accomplish a minimum repose time of *iSeg*, the multi-core architecture of today's computer systems is used. Therefore, all cost intensive process steps—*load image sequence*, *interactive semi-automatic AOI fitting*, *automatic AOI fitting* and *tailoring AOI*—are implemented for multithreading.

Assigning a thread for each frame proved to be inefficient, since creating a thread consumes more resources than we save by this method. To avoid this, *iSeg* detects the number of CPU cores available on the host system. Lists of tasks for each available core are created, which have approximately the same amount of work and can be executed separately. With these lists, a thread on each available core is started. In combination with other optimization features, like the computation of feature points only in a certain area, as described in section 3.2, *iSeg* provides a minimum response time for user interaction even in computational expensive processes. In order to avoid restrictions on special hardware or drivers, *iSeg* does not use specific GPU based multithreading techniques.

4 EXPERIMENTAL TESTS

While developing, the performance of *iSeg* was only evaluated on the car data set *01-car pursuit* (Kurzhals et al., 2014a). To test the reliability of *iSeg*'s process, we used three additional data sets. A representative sample frame of all data sets can be seen in Figure 1. As a test for highly dynamic boundaries, we chose the *03-dialog* (Kurzhals et al., 2014a), because face boundaries exhibit the desired rapid change. Further, we used frames $0-60$ of the *S1 L1 PET2009* video by Ferryman and Shahrokni (2009) and the *road*data set by Wu et al. (2014). We chose the last two videos to be able to compare our *iSeg* with *SAGTA*.

In the test series, the same objects were annotated with the use of *iSeg* as the existing annotation. To give an idea how long the annotation process using *iSeg* needs, the processing time is determined. The results, the number of annotated objects, and the processing time are summarized in Figure 6.

5 DISCUSSION AND CONCLUSION

As shown in Figure 6, the tool *iSeg* for polygon-shaped object annotation and segmentation works well on different scenarios. Comparing the processing time (annotation time) of *iSeg* on the road data set with the processing time of *SAGTA* (Wu et al., 2014), our approach takes 33*min* longer for creat-

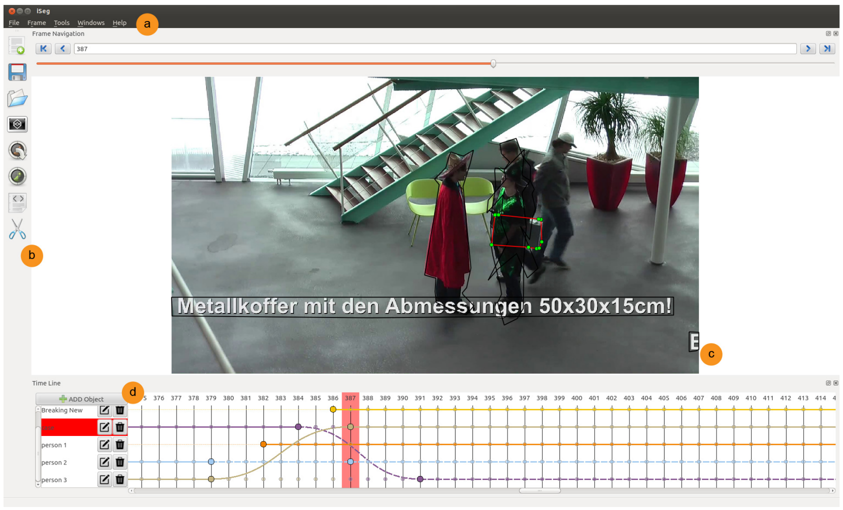

Figure 5: User interface of iSeg with its four main areas: ⓐ *main context menu*; ⓑ *tool bar*; ⓒ *frame view* and *navigation area*; ⓓ *semantic time line*.

	Original rectangular AOI		Resulting polygon AOI	Resulting minimal rectangular AOI	Resulting rectangular AOI
01-car pursuit (Kurzhals et al., 2014a)		**#objects:** 2 **time:** 22*min*	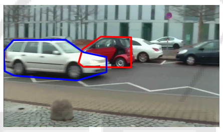	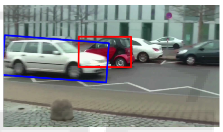	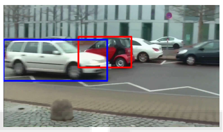
03-dialog (Kurzhals et al., 2014a)	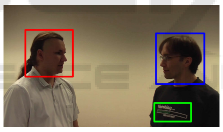	**#objects:** 3 **time:** 41*min*	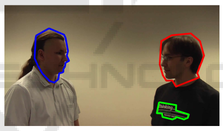	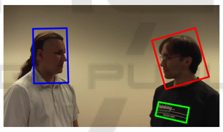	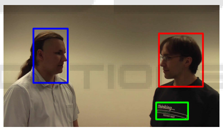
S1 L1 PET2009 (Ferryman and Shahrokni, 2009)	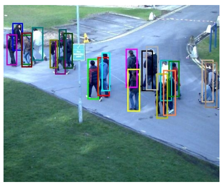	**#objects:** 11 **time:** 59*min*	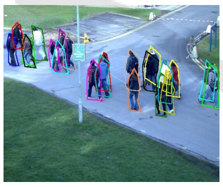	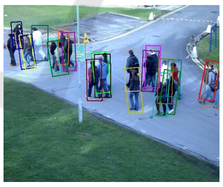	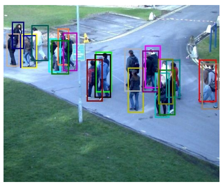
road (Wu et al., 2014)	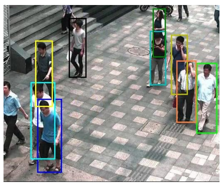	**#objects:** 10 **time:** 24*min*	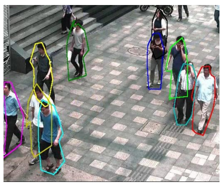	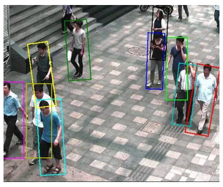	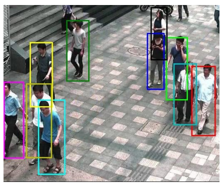

Figure 6: Resulting AOI using *iSeg*.

ing the annotations. But since polygon-shaped AOI contain much more information and are more accurate than rectangular AOI, this result is not surprising. A comparative evaluation based on polygon-shaped AOI was not possible for us. As stated above, *VIA* is the only video annotation tool, which should support polygon-shaped AOI (Dasiopoulou et al., 2011), but we did not find the option for it.

Polygonal annotation is clearly worth the trouble: Compared to rectangles, it allows for a much more precise description of the boundaries. A precise description of boundaries improves the 3D object reconstruction from video footage (Schöning, 2015) and for video inpainting. For other applications like the analysis of gaze data (Kurzhals et al., 2014b), which mostly depends on a rectangular description of the AOI, this rectangular description can easily be derived from the polygon description.

To overcome the still existing restrictions of our implementation, we will extend the activity diagram (Fig. 3) with components which detect deformation and rotation. Thus the affine transformation of the AOI can be improved significantly.

The current prototype of *iSeg* is *GPLv3* licensed and available online[2].

ACKNOWLEDGEMENTS

This work was funded by the German Research Foundation (DFG) as part of the Scalable Visual Analytics Priority Program (SPP 1335).

REFERENCES

Alt, H. and Guibas, L. J. (1996). Discrete geometric shapes: Matching, interpolation, and approximation: A survey. Technical report, Handbook of Computational Geometry.

Boykov, Y., Veksler, O., and Zabih, R. (2001). Fast approximate energy minimization via graph cuts. *IEEE Trans. Pattern Anal. Mach. Intell.*, 23(11):1222–1239.

Caselles, V., Kimmel, R., and Sapiro, G. (1997). Geodesic active contours. *Int J Comput Vision*, 22(1):61–79.

Cobos, F. and Peetre, J. (1991). Interpolation of compact operators: the multidimensional case. *Proc. Lond. Math. Soc.*, 3(2):371–400.

Dasiopoulou, S., Giannakidou, E., Litos, G., Malasioti, P., and Kompatsiaris, Y. (2011). A survey of semantic image and video annotation tools. *Lect Notes Comput Sc*, pages 196–239.

Doermann, D. and Mihalcik, D. (2000). Tools and techniques for video performance evaluation. *International Conference on Pattern Recognition*, 4:167 – 170.

Ferryman, J. and Shahrokni, A. (2009). PETs2009: Dataset and challenge. *IEEE International Workshop on Performance Evaluation of Tracking and Surveillance*.

Gotsman, C. and Surazhsky, V. (2001). Guaranteed intersection-free polygon morphing. *Comput Graph*, 25(1):67–75.

Höferlin, B., Höferlin, M., Heidemann, G., and Weiskopf, D. (2015). Scalable video visual analytics. *Inf Vis*, 14(1):10–26.

Kurzhals, K., Bopp, C. F., Bässler, J., Ebinger, F., and Weiskopf, D. (2014a). Benchmark data for evaluating visualization and analysis techniques for eye tracking for video stimuli. *Workshop on Beyond Time and Errors Novel Evaluation Methods for Visualization*.

Kurzhals, K., Heimerl, F., and Weiskopf, D. (2014b). Iseecube: visual analysis of gaze data for video. *Symposium on Eye Tracking Research and Applications*, pages 43–50.

Lowe, D. G. (2004). Distinctive image features from scale-invariant keypoints. *Int J Comput Vision*, 60(2):91–110.

Muja, M. and Lowe, D. G. (2009). Fast approximate nearest neighbors with automatic algorithm configuration. *International Conference on Computer Vision Theory and Applications*, 2:331–340.

Multimedia Knowledge and Social Media Analytics Laboratory (2015). Video image annotation tool. http://mklab.iti.gr/project/via.

Rother, C., Kolmogorov, V., and Blake, A. (2004). “GrabCut” interactive foreground extraction using iterated graph cuts. *ACM Trans Graph*, 23(3):309–314.

Rublee, E., Rabaud, V., Konolige, K., and Bradski, G. (2011). ORB: an efficient alternative to SIFT or SURF. *IEEE International Conference on Computer Vision*, pages 2564–2571.

Schöning, J. (2015). Interactive 3D reconstruction: New opportunities for getting cad-ready models. In *Imperial College Computing Student Workshop*, volume 49, pages 54–61. Schloss Dagstuhl–Leibniz-Zentrum fuer Informatik.

Schöning, J., Faion, P., and Heidemann, G. (2015). Semi-automatic ground truth annotation in videos: An interactive tool for polygon-based object annotation and segmentation. In *International Conference on Knowledge Capture*, pages 17:1–17:4. ACM, New York.

Schroeter, R., Hunter, J., and Kosovic, D. (2003). Vannotea - A collaborative video indexing, annotation and discussion system for broadband networks. *Workshop on Knowledge Markup & Semantic Annotation*,pages 1–8

Shneiderman, B. (1984). Response time and display rate in human performance with computers. *ACM Comput Surv*, 16(3):265–285.

Tanisaro, P., Schöning, J., Kurzhals, K., Heidemann, G., and Weiskopf, D. (2015). Visual analytics for video applications. *it-Information Technology*, 57:30–36.

Wu, S., Zheng, S., Yang, H., Fan, Y., Liang, L., and Su, H. (2014). Sagta: Semi-automatic ground truth annotation in crowd scenes. *IEEE International Conference on Multimedia and Expo Workshosps*.

Yao, A., Gall, J., Leistner, C., and Van Gool, L. (2012). Interactive object detection. *International Conference on Pattern Recognition*, pages 3242–3249.

YouTube (2015). Statistics - youtube: https://www.youtube.com/yt/press/statistics.html.

[2]Source code and binaries for *Ubuntu*, *Mac OS X* and *Windows*: https://ikw.uos.de/∼cv/projects/iSeg